



WILLIAMSON FLUID FLOW BEHAVIOUR OF MHD CONVECTIVE-RADIATIVE CATTANEO-CHRISTOV HEAT FLUX TYPE OVER A LINEARLY STRETCHED-SURFACE WITH HEAT GENERATION AND THERMAL-DIFFUSION

Md. Shakhaoath Khan^{a,*}, Md. Mizanur Rahman^{a, b}, S.M. Arifuzzaman^c, Pronab Biswas^c, Ifsana Karim^a

^a Discipline of Chemical Engineering, University of Newcastle, Callaghan NSW 2308, Australia

^b Department of Mathematics, Islamic University, Kushtia 7003, Bangladesh

^c Mathematics Discipline, Khulna University, Khulna 9208, Bangladesh

ABSTRACT

A two-dimensional (2D) flow of an incompressible Williamson fluid of Cattaneo-Christov heat flux type over a linearly stretched surface with the influence of magnetic field, thermal radiation-diffusion, heat generation and viscous dissipation is carried out in the present study. To develop a Williamson flow model, a boundary layer approximation is taken into account. The non-dimensional, nonlinear, coupled ordinary differential equations with boundary condition are solved numerically using Nactsheim-Swigert shooting iteration technique together with Runge-Kutta six order iteration scheme. The influences of physical parameters on the velocity, temperature, concentration is analysed through graphical consequences. To validate the accuracy of the numerical simulations scheme, comparisons is carried out with the previous studies and are found in an excellent agreement.

Keywords: Williamson fluid, Cattaneo-Christov heat flux, MHD, thermal radiation and diffusion, heat generation.

1. INTRODUCTION

Due to many applications in engineering industries, the magnetohydrodynamic (MHD) stretching sheet flow models are of great importance now days (Afify and Elgazery, 2016; Bég et al., 2014; Eid, 2016; Ferdows et al., 2012; Hayat et al., 2017; Khan et al., 2012; Mabood, Khan, and Ismail, 2015; Nayak et al., 2016; Reddy and Chamkha, 2016; Sreedevi et al., 2016). Such applications include liquid coating on photographic films, extrusion of polymer sheet from expire, boundary layer along liquid film concentration process, aerodynamic extrusion of plastic sheets, etc. In addition, a wide range of applications on MHD flow can be found in numerical fields such as electronic cooling, boilers, heat insulation and metal extrusion, liquid metal fluids oil reservoirs, geothermal systems, nuclear process, micro MHD pumps, high-temperature plasmas, ground water systems, energy storage units, biological transportation, thermal energy storage devices etc.

In recent years, the study of non-Newtonian fluids is of great attention for scientists (Abo-Eldahab and Salem, 2005; Asghar et al., 2007; El-Kabeir et al., 2008; Eldabe et al., 2012; Ezzat, 2010; Gaffar et al., 2015; Hameed and Nadeem, 2007; Hsiao et al., 2014; Jayachandra Babu and Sandeep, 2016; Khan et al., 2012; Rashidi et al., 2016; Rundora and Makinde, 2015; Si et al., 2016; Turkyilmazoglu, 2012; Umamaheswar et al., 2016) because of their various technical applications such as performance of lubricants, movement of biological fluids, sugar solutions, apple sauce, tomato ketchup, shampoos etc. To explain the behaviour of non-Newtonian fluid, different fluid models have been proposed where the pseudo-plastic fluids are of greatest communal. Examples of the fluids with pseudo-plastic features include power law model, Ellis model, Cross model, Carreaus model, and Williamson fluid

model. Among these Williamson fluid models get very little attention till date whilst this type of fluids can scientifically describe shear thinning non-Newtonian fluids flows. For example, blood, paint, ketchup, whipped cream, nail polish, polymer melts/solutions, etc. are the manufacturing and biological liquors that comply with the Williamson fluid. Williamson fluids are firstly introduced by Williamson (1929) in his pioneer research of Pseudo-plastic materials flow. He explained the flow of pseudo-plastic fluids by developing a model equation and verified this hypothesis with experiment. Nadeem and Akram (2010a); (Nadeem and Akram, 2010b) investigated the effect of presence of inclined magnetic field on peristaltic flow of a Williamson fluid in an inclined symmetric or asymmetric channel. Akbar, Hayat, Nadeem, and Obaidat (2012) studied partial slip and heat transfer peristaltic flow behaviour of a Williamson fluid through inclined asymmetric channel. This study was later extended by incorporating nanoparticle (Akbar et al., 2013). Vajravelu et al. (2012) analysed Williamson fluid flow (peristaltic) in asymmetric channels with permeable walls having different amplitudes and phases. They have also discussed the influence of various wave forms on the fluid flow pattern. Akram et al., (2013) investigated the influence of induced magnetic field on peristaltic flow of Williamson fluid flow by analytically as well as numerically. Bhatti and Rashidi (2016) shows the thermo-diffusion and thermal radiation effects of the flow pattern of Williamson nanofluid over a porous shrinking/stretching sheet. Recent studies in this are also includes various physical parameters such as pressure dependent viscosity (Zehra et al., 2015), Hall effects (Eldabe et al., 2016), melting heat transfer (Hayat et al., 2016), convective conditions of heat and mass transfer flow (Hayat et al., 2016), thermal radiation and Ohmic dissipation (Hayat et al., 2016), chemical reaction (Krishnamurthy et al., 2016), variable thickness (Salahuddin et al., 2016), bidirectional stretching surface of non-linear

* Corresponding author. Email: Md.S.Khan@newcastle.edu.au

type (Bilal et al., 2017), homogeneous–heterogeneous reactions (Ramzan et al., 2017).

Heat generation effects on fluid flow of boundary layer type is very significant due to engineering and industrial applications including reactor safety analysis, radioactive materials, spent nuclear fuel, fire and combustion, metal waste, etc. In recent years, investigators are more interested on heat generation dynamical effects (Abbas et al., 2016; Bararnia et al., 2009; Hady et al., 2006; Kataria and Patel, 2016; Khan et al., 2014; Khan and Mahmood, 2016; Li et al., 2016; Madhava Reddy et al., 2015; Mahmoud and Waheed, 2012; Srinivasa and Eswara, 2016; Zhang and Zheng, 2012). Reddy and Chamkha (2016) reported heat generation/absorption effects on MHD convective Al₂O₃–water and TiO₂–water nanofluids flow past a stretching sheet. The influence of heat generation on electrically conducting fluid flow towards an isothermal truncated cone was investigated by Srinivasa and Eswara (2016). Hayat et al. (2017) studied the MHD three-dimensional Oldroyd-B nanofluid flow with heat generation/absorption effects.

The influence of viscous dissipation on MHD heat and mass transfer flow has significant importance which led this topic more attractive to the researchers in very recent years (Hayat et al., 2016; Mabood et al., 2016; Metri et al., 2016). Srinivas, Reddy et al. (2016) studied viscous dissipation effect on MHD thermal-diffusion and diffusion-thermo fluid flow concerning expanding/contracting rotating porous disks. Ahmed et al., (2017) investigated the influence of viscous dissipation on MHD chemically reacted heat and mass transfer fluid flow over a vertical porous plate. Recently the effect of presence of viscous dissipation on Combined electrical MHD radiative Maxwell fluid flow was described by Hsiao (2017).

With the advancement of many transport process, density differences driven flow caused by temperature-concentration gradient and material composition is of significant importance. It is therefore desired to study the flow behaviour induced by concentration differences unconventionally or instantaneously with temperature differences. The temperature gradient led the formation of mass flux which is so called thermal-diffusion which plays an imperative role in the process of solar ponds, microstructure of the world oceans, biological systems, mass transport across biological membranes etc. Recently the effect of presence of thermal diffusion on various boundary layer systems carried out by the researchers (Ashraf et al., 2016; Pal et al., 2016; Sravanthi, 2016; Yadav et al., 2016; Zaidi and Mohyud-Din, 2016; Zhao et al., 2016). In recent years, researchers have taken the boundary layer several types of fluid flow such as ferro fluid (Ahmad and Iqbal, 2017), eyring Powell fluid (Ahmad et al., 2017), hyperbolic tangent fluid (Iqbal et al., 2017), second-grade fluid (Abbas et al., 2015), casson fluid (Ahmed et al., 2017), viscoelastic fluid (Iqbal et al., 2017) flow into account.

From the wide-ranging literature survey, it is noted that the problem of MHD radiative Cattaneo–Christov heat flux type Williamson fluid flow over a linearly stretched surface with the effect of heat generation, viscous dissipation and thermal-diffusion to the authors’ knowledge has not yet been explored. Therefore, this phenomenon is addressed in present study. The specific objectives of this numerical investigation are listed below:

- To develop a mathematical model to understand the MHD convective and radiative Cattaneo–Christov heat flux type Williamson fluid flow behaviour over a linearly stretched surface with the influence of heat generation, viscous dissipation and thermal-diffusion
- Numerical simulation of the flow governing model by employing Nactsheim-Swigert shooting iteration technique together with Runge-Kutta six order iteration scheme.
- Implementation of a code using FORTRAN Programming Language to elucidate the present problem.
- Validation of the numerical technique with available literature.

- Investigating the boundary layer heat and mass transfer Williamson fluid flow with incorporation of different physical parameter.

2. MATHEMATICAL MODEL OF FLOW

Two-dimensional heat and mass transfer flow of Williamson fluid with Cattaneo–Christov heat flux over a linearly stretched surface with convective boundary condition is considered in the presence of a uniform thermal radiation and magnetic field. The fluid is flowing in the x-direction which is taken along the plate and y-axis is normal to it. Magnetic field of strength B_0 is applied which is normal to the flow direction of Williamson fluid. Initially, it is considered that the plate and Williamson fluid is at rest at the similar temperature $T(=T_\infty)$ and concentration level $C(=C_\infty)$ at all points. At the plate, temperature and species concentration are T_w and C_w respectively whereas T_∞ and C_∞ are fluid temperature and concentration of uniform flow respectively. The physical configuration and co-ordinate system of the problem is presented in the following Fig. 1.

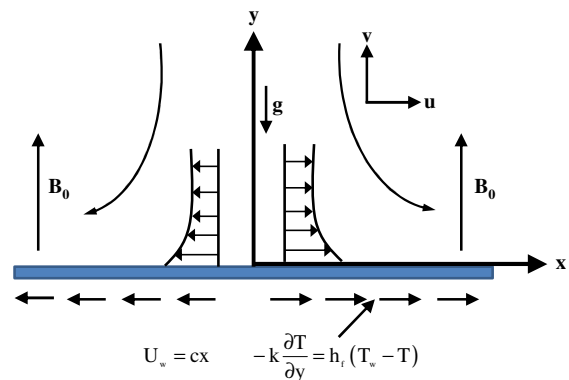


Fig. 1 Physical configuration and coordinate system.

2.1 Governing Equation

Under the assumptions made above, the governing boundary layer equations for MHD convective Williamson fluid flow behaviour of Cattaneo–Christov heat flux type over a linearly stretched surface with heat generation, viscous dissipation, thermal radiation and thermal diffusion, reduce to (Ramzan et al., 2017; Salahuddin et al., 2016):

Continuity equation

$$\frac{\partial u}{\partial x} + \frac{\partial v}{\partial y} = 0, \quad (1)$$

Momentum equation

$$u \frac{\partial u}{\partial x} + v \frac{\partial u}{\partial y} = u_e \left(\frac{dU_e}{dx} \right) + v \left(\frac{\partial^2 u}{\partial x^2} \right) + \sqrt{2} \Gamma v \left(\frac{\partial u}{\partial y} \right) \left(\frac{\partial^2 u}{\partial y^2} \right), \quad (2)$$

$$-\frac{\sigma B_0^2}{\rho} (u - u_e) + g \beta (T - T_\infty) + g \beta^* (C - C_\infty)$$

Energy equation

$$u \frac{\partial T}{\partial x} + v \frac{\partial T}{\partial y} = \frac{\kappa}{\rho c_p} \left(\frac{\partial^2 T}{\partial y^2} \right) - \lambda_1 \left[u^2 \left(\frac{\partial^2 T}{\partial x^2} \right) + 2uv \left(\frac{\partial^2 T}{\partial x \partial y} \right) + v^2 \left(\frac{\partial^2 T}{\partial y^2} \right) \right]$$

$$-\lambda_1 \left[\left(u \frac{\partial u}{\partial x} + v \frac{\partial u}{\partial y} \right) \left(\frac{\partial T}{\partial x} \right) + \left(u \frac{\partial v}{\partial x} + v \frac{\partial v}{\partial y} \right) \left(\frac{\partial T}{\partial y} \right) \right],$$

$$+ \frac{Q_0}{\rho c_p} (T - T_\infty) + \frac{v}{c_p} \left(\frac{\partial u}{\partial y} \right)^2 - \frac{1}{\rho c_p} \left(\frac{\partial q_r}{\partial y} \right) \quad (3)$$

Concentration equation

$$u \frac{\partial C}{\partial x} + v \frac{\partial C}{\partial y} = D_m \left(\frac{\partial^2 C}{\partial y^2} \right) + D_T \left(\frac{\partial^2 T}{\partial y^2} \right). \quad (4)$$

With boundary condition,

$$u = U_w = cx, v = 0, -k \frac{\partial T}{\partial y} = h_f (T_w - T), C = C_w \text{ at } y = 0 \quad (5)$$

$$u \rightarrow u_e = ax, T \rightarrow T_\infty, C \rightarrow C_\infty \text{ at } y \rightarrow \infty$$

Where, u and v are the velocity component in the x and y axis respectively, u_e is the variable external free stream velocity, B_0 is the magnetic field component, Γ is the time rate constant, β is thermal expansion coefficient, β^* is concentration expansion coefficient, ν is the kinematic viscosity, ρ is density, k is thermal conductivity, c_p is specific heat at constant pressure, Q_0 denotes the heat source, q_r unidirectional radiative heat flux, D_m is mass diffusion coefficient and D_T is the thermal diffusion coefficient.

The radiative heat flux term by using the Rosseland approximation (Perdikis and Raptis, 1996) is given by $q_r = -\frac{4\sigma^* \partial T^4}{3k^* \partial y}$. Where, σ^* is

the Stefan-Boltzmann constant and k^* is the mean absorption coefficient, respectively. If temperature differences within the flow are sufficiently small, then the q_r can be linearized by expanding T^4 into the Taylor series about T_∞ , which after neglecting higher order terms takes the form by $T^4 \cong 4T_\infty^3 T - 3T_\infty^4$.

2.2 Similarity solution

In order to attain a similarity solution to Eqs. (1)-(4) with the boundary conditions (Eq. (5)) the following dimensionless variables are used,

$$\eta = y \sqrt{\frac{c}{\nu}}, u = cx f'(\eta), v = -\sqrt{c\nu} f(\eta) \quad (6)$$

$$\theta = \theta(\eta) = \frac{T - T_\infty}{T_w - T_\infty}, \varphi = \varphi(\eta) = \frac{C - C_\infty}{C_w - C_\infty}$$

Continuity equation is satisfied. From the above transformations, the non-dimensional, nonlinear, coupled ordinary differential equations are obtained as:

$$f'''(\eta) + f(\eta) f''(\eta) - f'(\eta)^2 + W_e f''(\eta) f'''(\eta) - M [f'(\eta) - \lambda] + \lambda^2 + G_r \theta(\eta) + G_m \varphi(\eta) = 0 \quad (7)$$

$$\theta''(\eta) - P_r \gamma f(\eta)^2 \theta'(\eta) + R \theta''(\eta) + E_c P_r f''(\eta)^2 - P_r \gamma f(\eta) f'(\eta) \theta'(\eta) + P_r f(\eta) \theta'(\eta) + Q P_r \theta(\eta) = 0 \quad (8)$$

$$\varphi''(\eta) + S_0 S_c \theta''(\eta) + S_c f(\eta) \varphi'(\eta) = 0, \quad (9)$$

The transformed boundary conditions:

$$\left. \begin{aligned} f(0) = 0, f'(0) = 1, \theta'(0) = -\gamma_1 [1 - \theta(0)], \varphi(0) = 1 \text{ at } \eta = 0 \\ f'(\infty) \rightarrow \frac{a}{c}, \theta(\infty) \rightarrow 0, \varphi(\infty) \rightarrow 0 \text{ as } \eta \rightarrow \infty \end{aligned} \right\}, (10)$$

where the obtained physical parameters are given below:

Hartmann number, $M = \frac{\sigma B_0^2}{c\rho}$, Williamson fluid parameter,

$W_e = U_w \sqrt{\frac{2c}{\nu}} \Gamma$, Velocity ratio parameter, $\frac{a}{c}$, Grashof number,

$G_r = \frac{g\beta(T_w - T_\infty)}{cU_w}$, modified Grashof number $G_m = \frac{g\beta^*(C_w - C_\infty)}{cU_w}$,

Prandtl number, $P_r = \frac{\rho c_p \nu}{\kappa}$, Thermal relaxation time parameter, $\gamma = \lambda c$

, Biot number, $\gamma_1 = \frac{h_f}{k} \sqrt{\frac{\nu}{a}}$, Radiation parameter, $R = \frac{16 \sigma^* T_\infty^3}{3 k \kappa^*}$, heat

source parameter, $Q = \frac{Q_0}{c\rho c_p}$, Eckert number, $E_c = \frac{U_w^2}{c_p(T_w - T_\infty)}$,

Schmidt number, $S_c = \frac{\nu}{D_m}$, Soret number, $S_o = \frac{D_T}{\nu} \left(\frac{T_w - T_\infty}{C_w - C_\infty} \right)$.

2.3 Skin-friction coefficients, Nusselt and Sherwood Number at the sheet

The parameters of technological interest for the present problem are the local skin-friction ($C_{f,x}$), the local Nusselt number ($N_{u,x}$) and the local Sherwood number ($S_{h,x}$), which are elucidated as

$$C_{f,x} = \frac{\tau_w}{\rho U_w^2}; N_{u,x} = \frac{xq_w}{k(T_w - T_\infty)}; S_{h,x} = \frac{xq_m}{D_m(C_w - C_\infty)}, \quad (11)$$

where τ_w , q_w and q_m are respectively the wall shear stress, wall heat flux and wall mass flux, can be defined as:

$$\tau_w = \mu \frac{\partial u}{\partial y} \left[1 + \frac{\Gamma}{2} \left(\frac{\partial u}{\partial y} \right) \right]_{y=0}; q_w = -k \left(\frac{\partial T}{\partial y} \right)_{y=0}; q_m = -D_m \left(\frac{\partial C}{\partial y} \right)_{y=0} \quad (12)$$

In view of dimensionless variables (Eq. (6)) and above equation, the dimensionless forms of local skin friction coefficient, local Nusselt number and local Sherwood number can be written as follows:

$$2\sqrt{2} C_{f,x} \text{Re}_x^{1/2} = f''(0) + W_e f''(0) \quad (13)$$

$$N_{u,x} \text{Re}_x^{1/2} = -\theta'(0)$$

$$S_{h,x} \text{Re}_x^{1/2} = -\varphi'(0)$$

where $\text{Re}_x = \frac{xU_w}{\nu}$ is the Reynolds number.

3. NUMERICAL TECHNIQUE

The non-dimensional, nonlinear, coupled ordinary differential equations (Eqs. (7)-(9)) with boundary condition (Eq. (10)) are solved numerically using standard initially value solver the shooting method. For the purpose of this method, the Nactsheim-Swigert shooting iteration technique together with Runge-Kutta six order iteration scheme (Nachtsheim and Swigert, 1995) is taken and determines the temperature and concentration as a function of the coordinate η . Extension of the iteration shell to above equation system of differential Eq. (10) is straightforward, there are three asymptotic boundary condition and hence three unknown surface conditions $f''(0)$, $\theta'(0)$ and $\varphi'(0)$.

4. RESULTS AND DISCUSSION

The boundary layer heat and mass transfer laminar flow problem associated with the Williamson fluid of MHD Cattaneo-Christov heat flux type over a linearly stretched surface with heat generation, viscous dissipation and thermal-diffusion has been studied numerically. In order to investigate the physical representation of the problem, the numerical values of velocity ($f'(\eta)$), temperature ($\theta(\eta)$) and species concentration ($\varphi(\eta)$) with the boundary layer have been computed for different parameters as Williamson fluid parameter, W_e , Grashof number, G_r , modified Grashof number, G_c , Hartmann number, M , velocity ratio

parameter, a/c , Prandtl number, Pr , thermal radiation, R , heat source, Q , Eckert number, E_c , Schmidt number, S_c and Soret number, S_o . In order to assess the accuracy of the numerical results the present results are compared with the previous studies (Fang et al., 2009; Nadeem et al., 2013; Ramzan et al., 2017; Salahuddin et al., 2016; Sher Akbar et al., 2015) presented in Tables 1-3 and excellent agreement is observed. To study the various parameter effects on Williamson fluid flow field, the velocity, temperature and concentration profiles are shown in Figs. 2-16.

Table 1 Comparison of skin friction coefficient for different values of Williamson fluid parameter (W_e) when $M=a/c=G_r=G_m=\gamma_1=P_r=R=E_c=Q=S_0=S_c=0$.

W_e	Nadeem et al. (2013)	Ramzan et al. (2017)	Present
0.0	1.0	1.0	1.0
0.1	0.976588	0.976586	0.976589
0.2	0.939817	0.939814	0.939818
0.3	0.88272	0.88270	0.88271

Table 2 Comparison of skin friction coefficient for different values of Hartmann number (M) when $W_e=a/c=G_r=G_m=\gamma_1=P_r=R=E_c=Q=S_0=S_c=0$.

M	Fang et al. (2009)	Sher Akbar et al. (2015)	Salahuddin et al. (2016)	Present
0		1.0	1.0	1.0
0.5		-1.11803	-1.11801	-1.11810
1		-1.41421	-1.41418	-1.41423
5		-2.44949	-2.44942	-2.44951
10		-3.31663	-3.31656	-3.31667
100	-1.1180	-10.04988	-10.04981	-10.04990
500		-22.38303	-22.38293	-22.38307
1000		-31.63839	-31.63846	-31.63841

Table 3. Comparison of Nusselt number for different values of Prandtl number (Pr) when $W_e=M=a/c=G_r=G_m=\gamma_1=R=E_c=Q=S_0=S_c=0$.

Pr	Wang (1989)	Mabood et al. (2015)	Salahuddin et al. (2016)	Present
0.07	0.0656	0.0655	0.0654	0.0659
0.20	0.1691	0.1691	0.1688	0.1696
0.70	0.4539	0.4539	0.4534	0.4542
2.00	0.9114	0.9114	0.9108	0.9117
7.00	1.8954	1.8954	1.8944	1.8959
20.00	3.3539	3.3539	3.3522	3.3543
70.00	6.4622	6.4622	6.4619	6.4624

The velocity field of the Williamson fluid for different parametric effects are given in Figs. 2-7.

Fig. 2 shows the effect of presence of different Hartmann number parameter, M , on velocity profile where the other parameters were set aside as $W_e=0.1, P_r=2.0, G_r=2.0, G_m=0.5, \gamma_1=0.2, R=2.0, E_c=0.003, Q=2.5, S_0=1.5$ and $S_c=0.9$. It can be seen that, the increasing effect of M led the velocity profile decreases. This behaviour could be attributed to amplified Lorentz force where the increasing effect of Hartmann number is opposing the motion of the Williamson fluid and therefore velocity profile decreases.

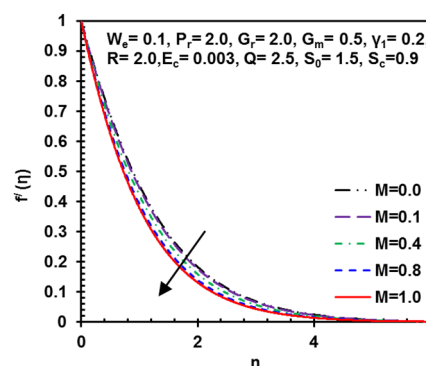


Fig. 2 Variation of velocity profile ($f'(\eta)$) for different values of Hartmann number, M .

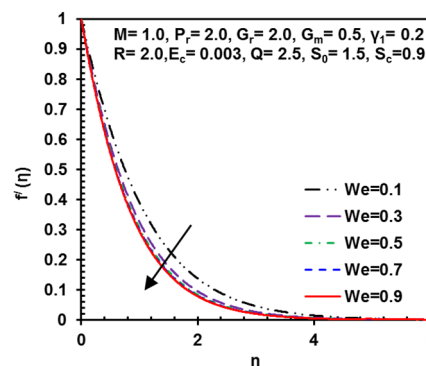


Fig. 3 Variation of velocity profile ($f'(\eta)$) for different values of Williamson fluid parameter, W_e .

The velocity profile for different values of Williamson fluid parameter, W_e , are given in Fig. 3 which shows a decreasing trend in momentum boundary layer due to increase in W_e . The additional parameters were kept as $M=1.0, P_r=2.0, G_r=2.0, G_m=0.5, \gamma_1=0.2, R=2.0, E_c=0.003, Q=2.5, S_0=1.5$ and $S_c=0.9$. This behaviour could be attributed due to the higher resistance to the flow of Williamson fluid.

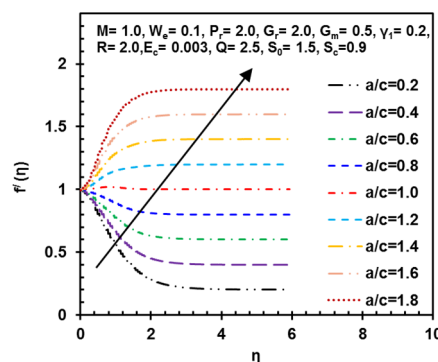


Fig. 4 Variation of velocity profile ($f'(\eta)$) for different values of velocity ratio parameter, a/c .

Fig. 4 gives the different velocity ratio parameter, a/c , effects on velocity profile where the other parameters were set aside as $M=1.0, W_e=0.1, P_r=2.0, G_r=2.0, G_m=0.5, \gamma_1=0.2, R=2.0, E_c=0.003, Q=2.5, S_0=1.5$ and $S_c=0.9$. It is observed that the distribution of the velocity of Williamson fluid is an increasing function of velocity ratio parameter. The boundary condition of the corresponding profile precisely matches. This profile is also physically important because of it provides

information when the velocity of the stretching sheet's is greater than the velocity of the free stream.

The velocity profile for different values of Grashof number, G_r , are given in Fig. 5. The additional parameters were kept as $M=1.0$, $P_r=2.0$, $G_m=0.5$, $\gamma_1=0.2$, $R=2.0$, $E_c=0.003$, $Q=2.5$, $S_0=1.5$ and $S_c=0.9$. An increase in G_r parameter is observed to strappingly accelerate the flow of Williamson fluid. The heightening in thermal buoyancy forces assistances momentum growth since $G_r \theta(\eta)$ is an assistive body force ascending in the momentum equation (Eq. (7)) and this will assistance viscous diffusion and hence increase velocities. This effect is continued for all distances slanting from the stretching sheet to the free stream.

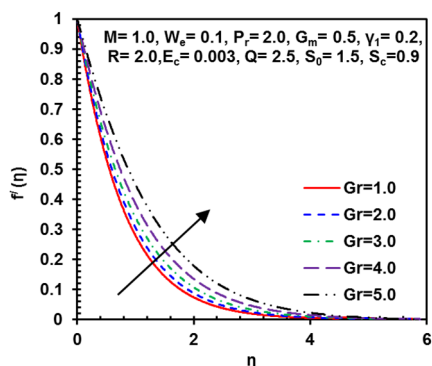


Fig. 5 Variation of velocity profile ($f'(\eta)$) for different values of Grashof number, G_r .

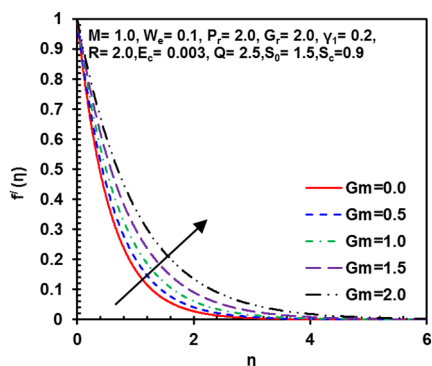


Fig. 6 Variation of velocity profile ($f'(\eta)$) for different values of modified Grashof number, G_m .

Fig. 6 shows the velocity distribution for different values of modified Grashof number, G_m , where $M=1.0$, $W_e=0.1$, $P_r=2.0$, $G_r=2.0$, $\gamma_1=0.2$, $R=2.0$, $E_c=0.003$, $Q=2.5$, $S_0=1.5$ and $S_c=0.9$. It can be seen that, increasing modified Grashof number (mass convective/ species buoyancy) effect led the flow accelerated and increase the momentum boundary layer. This behaviour occurred because of effect of riding species buoyancy force which aids increases boundary layer thickness further from the sheet.

The variation of velocity profile for different values of Eckert number, E_c , is shown in Fig. 7 where $M=1.0$, $W_e=0.1$, $P_r=2.0$, $G_r=2.0$, $G_m=0.5$, $\gamma_1=0.2$, $R=2.0$, $Q=2.5$, $S_0=1.5$ and $S_c=0.9$. It is observed that the velocity distribution is an increasing function of Eckert number. This is because the stretching sheet is being strained the viscous heating effect varies with distance into the boundary layer.

The temperature field of the Williamson fluid for different physical parameter effects are given in Figs. 8-12. The temperature distribution for different values of Williamson fluid parameter, W_e , are given in Fig. 8 where $M=1.0$, $P_r=2.0$, $G_r=2.0$, $G_m=0.5$, $\gamma_1=0.2$, $R=2.0$, $E_c=0.003$, $Q=2.5$, $S_0=1.5$ and $S_c=0.9$. An increasing trend in momentum boundary layer is observed due to increase in W_e . This behaviour could be attributed to the higher resistance and further molecular collisions in the Williamson fluid.

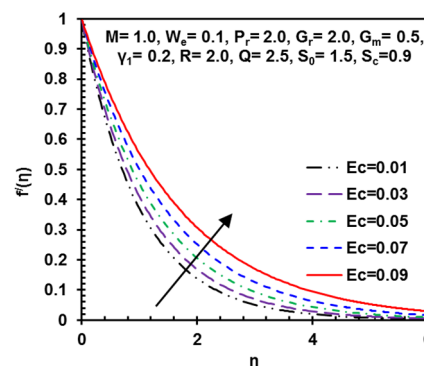


Fig. 7 Variation of velocity profile ($f'(\eta)$) for different values of Eckert number, E_c .

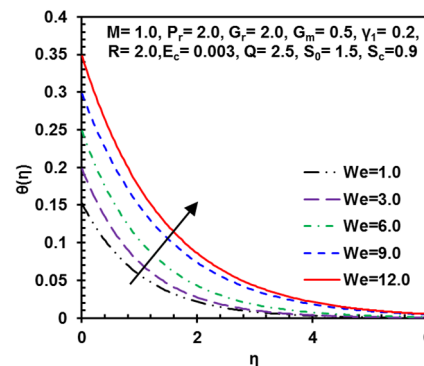


Fig. 8 Variation of temperature profile ($\theta(\eta)$) for different values of Williamson fluid parameter, W_e .

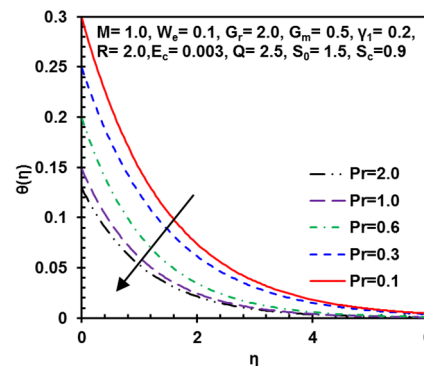


Fig. 9 Variation of temperature profile ($\theta(\eta)$) for different values of Prandtl number, P_r .

Fig. 9 portrayed the effect of Prandtl number, P_r , on temperature distribution where $M=1.0$, $W_e=0.1$, $G_r=2.0$, $G_m=0.5$, $\gamma_1=0.2$, $R=2.0$, $E_c=0.003$, $Q=2.5$, $S_0=1.5$ and $S_c=0.9$. It is evident that the temperature distribution is a decreasing function of Prandtl number. This is because the thermal diffusivity of the fluid is decreases due to higher values of P_r which further led the reduction in the thermal boundary layer thickness.

The temperature profile for different values of Eckert number, E_c , is displayed in Fig. 10 where $M=1.0$, $W_e=0.1$, $P_r=2.0$, $G_r=2.0$, $G_m=0.5$, $\gamma_1=0.2$, $R=2.0$, $Q=2.5$, $S_0=1.5$ and $S_c=0.9$. It is noticed that temperature profile shows increasing effect for higher Eckert number. Because further from the wall however increasing E_c turns to noticeably increase temperature values and therefore the temperature boundary layer thickness increases.

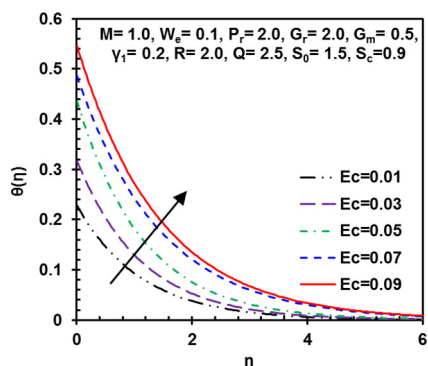


Fig. 10 Variation of temperature profile ($\theta(\eta)$) for different values of Eckert number, E_c .

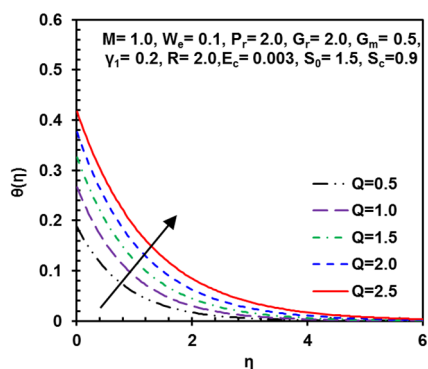


Fig. 11 Variation of temperature profile ($\theta(\eta)$) for different values of Heat source parameter, Q .

Fig. 11 displayed the heat source parameter, Q , effects on temperature distribution for $M=1.0$, $W_e=0.1$, $P_r=2.0$, $G_r=2.0$, $G_m=0.5$, $\gamma_1=0.2$, $R=2.0$, $E_c=0.003$, $S_0=1.5$ and $S_c=0.9$. It is apparent that the temperature profile is an increasing function of heat source parameter. Therefore, the increase in Q led the increase in thermal boundary layer thickness.

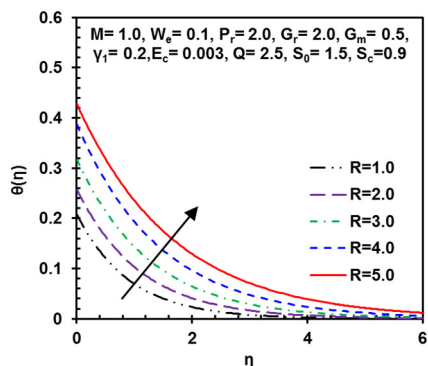


Fig. 12 Variation of temperature profile ($\theta(\eta)$) for different values of radiation parameter, R .

The temperature profile for different values of thermal radiation parameter, R , is shown in Fig. 12 where $M=1.0$, $W_e=0.1$, $P_r=2.0$, $G_r=2.0$, $G_m=0.5$, $\gamma_1=0.2$, $E_c=0.003$, $Q=2.5$, $S_0=1.5$ and $S_c=0.9$. It is perceived that the temperature in the Williamson fluid is markedly enhanced for higher radiation parameter. The radiation parameter is basically representing the relative influence of thermal radiation heat transfer to thermal conduction heat transfer. In the time being thermal radiation enhances the thermal diffusivity of the Williamson fluid, for growing values of thermal radiation parameter heat will be further added

to the system to the regime and therefore thermal boundary layer thickness will be increased.

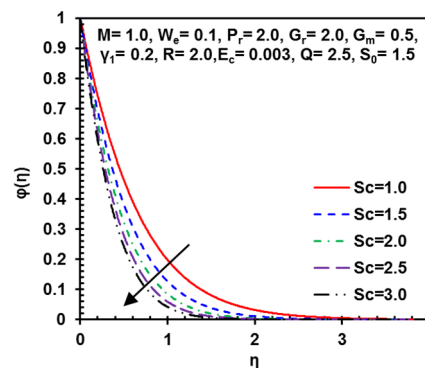


Fig. 13 Variation of concentration profile ($\phi(\eta)$) for different values of Schmidt number, S_c .

Figs. 13-16 display the influence of Schmidt number, S_c , Soret number, S_0 , Williamson fluid parameter, W_e and modified Grashof number, G_m respectively, on Williamson fluid concentration distributions.

A strong decrease in the Williamson fluid concentration is caused by increasing S_c in Fig. 13. Where the other parameters were set aside as $M=1.0$, $W_e=0.1$, $P_r=2.0$, $G_r=2.0$, $G_m=0.5$, $\gamma_1=0.2$, $R=2.0$, $E_c=0.003$, $Q=2.5$ and $S_0=1.5$. Furthermore, the increase of Schmidt number represents a decrease in dispersion of molecules (mass diffusion), the mass transfer rate is also decreases as S_c increases. Therefore, the concentration boundary layer thickness decreases, which led the reduction in $\phi(\eta)$.

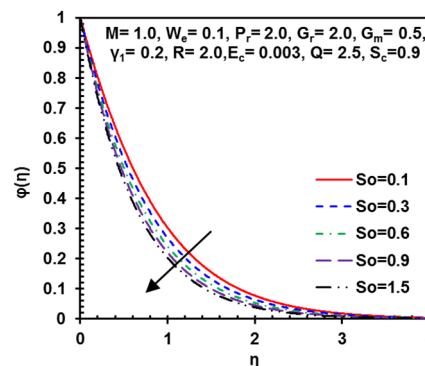


Fig. 14 Variation of concentration profile ($\phi(\eta)$) for different values of Soret number, S_0 .

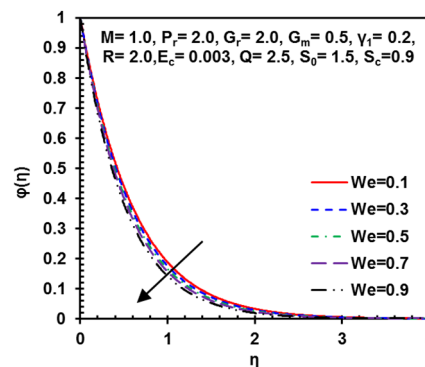


Fig. 15 Variation of concentration profile ($\phi(\eta)$) for different values of Williamson fluid parameter, W_e .

Fig. 14 shows Williamson fluid concentration is significantly decreases with increasing in Soret number, S_o where $M=1.0$, $W_e=0.1$, $P_r=2.0$, $G_r=2.0$, $G_m=0.5$, $\gamma_1=0.2$, $R=2.0$, $E_c=0.003$, $Q=2.5$ and $S_c=0.9$. This is due to the fact that destructive thermal diffusion diminishes the boundary layer thickness and increases the mass transfer.

An increase in the Soret number results a decrease in the concentration distribution within the boundary layer (Fig. 15) where the other parameters were fixed as $M=1.0$, $P_r=2.0$, $G_r=2.0$, $G_m=0.5$, $\gamma_1=0.2$, $R=2.0$, $E_c=0.003$, $Q=2.5$, $S_o=1.5$ and $S_c=0.9$. This behaviour can be attributed to the fact that significant molecular collisions in the Williamson fluid and furthermore, higher resistance in the system led concentration boundary layer thickness decreases.

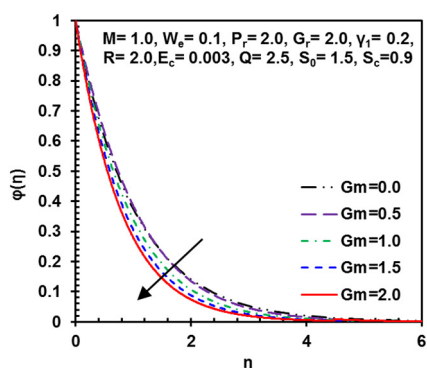


Fig. 16 Variation of concentration profile ($\phi(\eta)$) for different values of modified Grashof number, G_m .

Fig. 16 exhibits the increasing effect of modified Grashof number, G_m , in the concentration distribution of Williamson fluid, where $M=1.0$, $W_e=0.1$, $P_r=2.0$, $G_r=2.0$, $\gamma_1=0.2$, $R=2.0$, $E_c=0.003$, $Q=2.5$, $S_o=1.5$ and $S_c=0.9$. It can be seen that the concentration profile gradually decreases due to increase in G_m . This is because the concentration boundary layer thickness is consequently dropped with increasing species buoyancy force which further led the reduction in $\phi(\eta)$.

5. CONCLUDING REMARKS

Present study numerically investigates laminar boundary layer heat and mass transfer Williamson fluid flow of Cattaneo–Christov heat flux type over a linearly stretched surface with the effect of heat generation, viscous dissipation, thermal radiation and thermal diffusion. The Nactsheim-Swigert shooting iteration technique together with Runge-Kutta six order iteration scheme was used to solve the transformed, non-dimensional two-point boundary value problem. The present numerical model was validated previously published literature. The following observations has been noticed in the present computations:

- The momentum boundary layer thickness was found to be enhances due to increase in Grashof number, modified Grashof number, Eckert number and velocity ratio parameter individually (generally accelerates the flow) whilst the Hartmann number and the Williamson fluid parameter deaccelerates the flow separately and therefore velocity profile decreases.
- The thermal boundary layer thickness and heat transfer rates were observed to be enhances due to increasing Williamson fluid parameter, Eckert number, thermal radiation and heat source parameter independently (generally accelerates the flow). However, the thermal boundary layer thickness decreases with increase in Prandtl number.
- The concentration distribution of fluid was found to be decrease due to increase in Schmidt number, Soret number, Williamson fluid parameter and modified Grashof number.

NOMENCLATURE

B_o	magnetic component, [$Wb\ m^{-2}$]
C_f	skin-friction, [-]
C_p	specific heat at constant pressure, [$J\ kg^{-1}\ K^{-1}$]
Da	Darcy number, [-]
D_m	mass diffusion coefficient, [$m^2\ s^{-1}$]
D_T	thermal diffusion coefficient, [$m^2\ s^{-1}$]
E_c	Eckert number, [-]
f'	dimensionless velocity, [-]
G_r	Grashof number, [-]
G_c	modified Grashof number, [-]
M	Hartmann number, [-]
P_r	Prandtl number, [-]
q_r	unidirectional radiative heat flux, [$kg\ m^{-2}$]
Q	heat source parameter, [-]
R	Radiation parameter
S_c	Schmidt number, [-]
S_o	Soret number, [-]
Sh	Sherwood number, [-]
T	Fluid temperature, [K]
T_w	Temperature at the plate surface, [K]
T_∞	ambient temperature as y tends to infinity, [K]
U_o	uniform velocity, [$m\ s^{-1}$]
u, v	velocity components, [$m\ s^{-1}$]
W_e	Williamson fluid parameter, [-]
x, y	Cartesian co-ordinates
<i>Greek symbols</i>	
ρ	density of the fluid, [$kg\ m^{-3}$]
μ	dynamic viscosities, [$kg\ m^{-1}\ s^{-1}$]
ν	kinematic viscosity, [$m^2\ s^{-1}$]
β	thermal expansion co-efficient
β^*	concentration expansion co-efficient
κ	thermal conductivity, ($W\ m^{-1}\ K^{-1}$)
σ_s	Stefan-Boltzmann constant, $5.6697 \times 10^{-8}\ [W\ m^{-2}\ K^{-4}]$
γ	Thermal relaxation time parameter, [-]
γ_1	Biot number, [-]
θ	dimensionless temperature
ϕ	dimensionless concentration

REFERENCES

- Abbas, Z., Ahmad, B., Ali, S., (2015), "Chemically Reactive Hydromagnetic Flow of a Second-Grade Fluid in a Semi-Porous Channel," *Journal of applied mechanics and technical physics*, **56**, 878–888.
<http://dx.doi.org/10.1134/S0021894415050156>
- Abbas, Z., Naveed, M., and Sajid, M., 2016, "Hydromagnetic Slip Flow of Nanofluid Over a Curved Stretching Surface with Heat Generation and Thermal Radiation," *Journal of Molecular Liquids*, **215**, 756-762.
<http://dx.doi.org/10.1016/j.molliq.2016.01.012>
- Abo-Eldahab, E.M., and Salem, A.M., 2005, "MHD Free-Convection Flow of a Non-Newtonian Power-Law Fluid at a Stretching Surface with A Uniform Free-Stream," *Applied Mathematics and Computation*, **169**(2), 806-818.
<http://dx.doi.org/10.1016/j.amc.2004.09.089>
- Afify, A.A., and Elgazery, N.S., 2016, "Effect of a Chemical Reaction on Magnetohydrodynamic Boundary Layer Flow of a Maxwell Fluid Over a Stretching Sheet with Nanoparticles," *Particuology*, **29**, 154-161.
<http://dx.doi.org/10.1016/j.partic.2016.05.003>

Ahmed, S., Zueco, J., and López-González, L.M., 2017, "Effects of Chemical Reaction, Heat and Mass Transfer and Viscous Dissipation Over a MHD Flow in a Vertical Porous Wall Using Perturbation Method," *International Journal of Heat and Mass Transfer*, **104**, 409-418.

<http://dx.doi.org/10.1016/j.ijheatmasstransfer.2016.07.076>

Ahmad, B., Iqbal, Z., (2017), "Framing the Performance of Variation in Resistance on Viscous Dissipative Transport of Ferro Fluid with Homogeneous and Heterogeneous Reactions," *Journal of Molecular Liquids*, **241**, 904-911.

<https://doi.org/10.1016/j.molliq.2017.06.077>

Ahmad, B., Iqbal, Z., (2017), "An Effect of Cattaneo Christov Heat Flux Model for Eyring Powell Fluid over an Exponentially Stretching Sheet," *Frontiers in heat and mass transfer*, **8**, 1-6.

<https://doi.org/10.5098/hmt.8.22>

Ahmed, B., Iqbal, Z., Azhar, E., (2017), "Combined Effects of Internal Heat Generation and Mass Effects on MHD Casson Fluid with Convective Boundary Conditions," *International Journal of Applied Electromagnetics and Mechanics*, **54**, 211-221.

<http://dx.doi.org/10.3233/JAE-160080>

Akbar, N.S., Hayat, T., Nadeem, S., and Obaidat, S., 2012, "Peristaltic Flow of a Williamson Fluid in an Inclined Asymmetric Channel with Partial Slip and Heat Transfer," *International Journal of Heat and Mass Transfer*, **55**(7), 1855-1862.

<http://dx.doi.org/10.1016/j.ijheatmasstransfer.2011.11.038>

Akbar, N.S., Nadeem, S., Lee, C., Khan, Z.H., and Haq, R.U., 2013, "Numerical Study of Williamson Nano Fluid Flow in an Asymmetric Channel," *Results in Physics*, **3**, 161-166.

<http://dx.doi.org/10.1016/j.rinp.2013.08.005>

Akram, S., Nadeem, S., and Hanif, M., 2013, "Numerical and Analytical Treatment on Peristaltic Flow of Williamson Fluid in the Occurrence of Induced Magnetic Field," *Journal of Magnetism and Magnetic Materials*, **346**, 142-151.

<http://dx.doi.org/10.1016/j.jmmm.2013.07.014>

Asghar, S., Hanif, K., Hayat, T., and Khaliq, C.M., 2007, "MHD Non-Newtonian Flow Due to Non-Coaxial Rotations of An Accelerated Disk and a Fluid at Infinity," *Communications in Nonlinear Science and Numerical Simulation*, **12**(4), 465-485.

<http://dx.doi.org/10.1016/j.cnsns.2005.04.006>

Bararnia, H., Ghotbi, A.R., and Domairry, G., 2009, "On the Analytical Solution for MHD Natural Convection Flow and Heat Generation Fluid in Porous Medium," *Communications in Nonlinear Science and Numerical Simulation*, **14**(6), 2689-2701.

<http://dx.doi.org/10.1016/j.cnsns.2008.09.018>

Bég, O.A., Khan, M.S., Karim, I., Alam, M.M., and Ferdows, M., 2014, "Explicit Numerical Study of Unsteady Hydromagnetic Mixed Convective Nanofluid Flow from an Exponentially Stretching Sheet in Porous Media," *Applied Nanoscience*, **4**(8), 943-957.

<http://dx.doi.org/10.1007/s13204-013-0275-0>

Bhatti, M.M., and Rashidi, M.M., 2016, "Effects of Thermo-Diffusion and Thermal Radiation on Williamson Nanofluid over a Porous Shrinking/Stretching Sheet," *Journal of Molecular Liquids*, **221**, 567-573.

<http://dx.doi.org/10.1016/j.molliq.2016.05.049>

Bilal Ashraf, M., Hayat, T., Alsaedi, A., and Shehzad, S.A., 2016, "Soret and Dufour Effects on the Mixed Convection Flow of an Oldroyd-B Fluid with Convective Boundary Conditions," *Results in Physics*, **6**, 917-924.

<http://dx.doi.org/10.1016/j.rinp.2016.11.009>

Bilal, S., Khalilur, R., Malik, M.Y., Hussain, A., and Khan, M., 2017, "Effects of Temperature Dependent Conductivity and Absorptive/Generative Heat Transfer on MHD Three Dimensional Flow Of Williamson Fluid Due To Bidirectional Non-Linear Stretching Surface," *Results in Physics*, **7**, 204-212.

<http://dx.doi.org/10.1016/j.rinp.2016.11.063>

Eid, M.R., 2016, "Chemical Reaction Effect on MHD Boundary-Layer Flow of Two-Phase Nanofluid Model over an Exponentially Stretching Sheet with a Heat Generation," *Journal of Molecular Liquids*, **220**, 718-725.

<http://dx.doi.org/10.1016/j.molliq.2016.05.005>

El-Kabeir, S.M.M., El-Hakiem, M.A., and Rashad, A.M., 2008, "Group Method Analysis of Combined Heat and Mass Transfer by MHD Non-Darcy Non-Newtonian Natural Convection Adjacent to Horizontal Cylinder in a Saturated Porous Medium," *Applied Mathematical Modelling*, **32**(11), 2378-2395.

<http://dx.doi.org/10.1016/j.apm.2007.09.013>

Eldabe, N.T., Elogail, M.A., Elshaboury, S.M., and Hasan, A.A., 2016, "Hall Effects on The Peristaltic Transport of Williamson Fluid Through a Porous Medium with Heat and Mass Transfer," *Applied Mathematical Modelling*, **40**(1), 315-328.

<http://dx.doi.org/10.1016/j.apm.2015.04.043>

Eldabe, N.T.M., Sallam, S.N., and Abou-zeid, M.Y., 2012, "Numerical Study of Viscous Dissipation Effect on Free Convection Heat and Mass Transfer of MHD Non-Newtonian Fluid Flow Through a Porous Medium," *Journal of the Egyptian Mathematical Society*, **20**(2), 139-151.

<http://dx.doi.org/10.1016/j.joems.2012.08.013>

Ezzat, M.A., 2010, "Thermoelectric MHD Non-Newtonian Fluid with Fractional Derivative Heat Transfer," *Physica B: Condensed Matter*, **405**(19), 4188-4194.

<http://dx.doi.org/10.1016/j.physb.2010.07.009>

Fang, T., Zhang, J., and Yao, S., 2009, "Slip MHD Viscous Flow over a Stretching Sheet – An Exact Solution," *Communications in Nonlinear Science and Numerical Simulation*, **14**(11), 3731-3737.

<http://dx.doi.org/10.1016/j.cnsns.2009.02.012>

Ferdows, M., Khan, M.S., Alam, M.M., and Sun, S., 2012, "MHD Mixed Convective Boundary Layer Flow of a Nanofluid through a Porous Medium Due to an Exponentially Stretching Sheet," *Mathematical problems in Engineering*, **3**(7), 1-21.

<http://dx.doi.org/10.1155/2012/408528>

Gaffar, S.A., Prasad, V.R., and Bég, O.A., 2015, "Numerical Study of Flow and Heat Transfer of Non-Newtonian Tangent Hyperbolic Fluid from a Sphere with Biot Number Effects," *Alexandria Engineering Journal*, **54**(4), 829-841.

<http://dx.doi.org/10.1016/j.aej.2015.07.001>

Hady, F.M., Mohamed, R.A., and Mahdy, A., 2006, "MHD Free Convection Flow along a Vertical Wavy Surface with Heat Generation or Absorption Effect," *International Communications in Heat and Mass Transfer*, **33**(10), 1253-1263.

<http://dx.doi.org/10.1016/j.icheatmasstransfer.2006.06.007>

Hameed, M., and Nadeem, S., 2007, "Unsteady MHD Flow of a Non-Newtonian Fluid on a Porous Plate," *Journal of Mathematical Analysis and Applications*, **325**(1), 724-733.

<http://dx.doi.org/10.1016/j.jmaa.2006.02.002>

Hayat, T., Bashir, G., Waqas, M., and Alsaedi, A., 2016, "MHD 2D Flow of Williamson Nanofluid Over a Nonlinear Variable Thickened Surface with Melting Heat Transfer," *Journal of Molecular Liquids*, **223**, 836-844.

<http://dx.doi.org/10.1016/j.molliq.2016.08.104>

Hayat, T., Bibi, S., Rafiq, M., Alsaedi, A., and Abbasi, F.M., 2016, "Effect of an Inclined Magnetic Field on Peristaltic Flow of Williamson Fluid in an Inclined Channel with Convective Conditions," *Journal of Magnetism and Magnetic Materials*, **401**, 733-745.

<http://dx.doi.org/10.1016/j.jmmm.2015.10.107>

Hayat, T., Imtiaz, M., and Alsaedi, A., 2016, "Melting Heat Transfer in The MHD Flow of Cu-Water Nanofluid With Viscous Dissipation and Joule Heating," *Advanced Powder Technology*, **27**(4), 1301-1308.

<http://dx.doi.org/10.1016/j.apt.2016.04.024>

Hayat, T., Muhammad, T., Shehzad, S.A., and Alsaedi, A., 2017, "An Analytical Solution for Magnetohydrodynamic Oldroyd-B Nanofluid Flow Induced by a Stretching Sheet with Heat Generation/Absorption," *International Journal of Thermal Sciences*, **111**, 274-288.

<http://dx.doi.org/10.1016/j.ijthermalsci.2016.08.009>

Hayat, T., Shafiq, A., and Alsaedi, A., 2016, "Hydromagnetic Boundary Layer Flow of Williamson Fluid in the Presence of Thermal Radiation and Ohmic Dissipation," *Alexandria Engineering Journal*, **55**(3), 2229-2240.

<http://dx.doi.org/10.1016/j.aej.2016.06.004>

Hsiao, C.Y., Chang, W.J., Char, M.I., and Tai, B.C., 2014, "Influence of Thermophoretic Particle Deposition on MHD Free Convection Flow of Non-Newtonian Fluids from a Vertical Plate Embedded in Porous Media Considering Soret and Dufour Effects," *Applied Mathematics and Computation*, **244**, 390-397.

<http://dx.doi.org/10.1016/j.amc.2014.07.007>

Hsiao, K.L., 2017, "Combined Electrical MHD Heat Transfer Thermal Extrusion System Using Maxwell Fluid with Radiative and Viscous Dissipation Effects," *Applied Thermal Engineering*, **112**, 1281-1288.

<http://dx.doi.org/10.1016/j.applthermaleng.2016.08.208>

Iqbal, Z., Azhar, E., Maraj, E.N., Ahmad, B., (2017), "Influence of Cattaneo-Christov Heat Flux Model on MHD Hyperbolic Tangent Fluid over a Moving Porous Surface," *Frontiers in Heat and Mass Transfer*, **8**, 1-7.

<http://dx.doi.org/10.5098/hmt.8.25>

Iqbal, Z., Mehmood, Z., Ahmed, B., (2017), "Elastic Deformation Analysis on MHD Viscous Dissipative Flow of Viscoelastic Fluid: An Exact Approach," *communication theoretical physics*, **67**, 561-567.

<http://dx.doi.org/10.1088/0253-6102/67/5/561>

Jayachandra B.M., and Sandeep, N., 2016, "MHD Non-Newtonian Fluid Flow over a Slendering Stretching Sheet in the Presence of Cross-Diffusion Effects," *Alexandria Engineering Journal*, **55**(3), 2193-2201.

<http://dx.doi.org/10.1016/j.aej.2016.06.009>

Kataria, H.R., and Patel, H.R., 2016, "Soret And Heat Generation Effects on MHD Casson Fluid Flow Past an Oscillating Vertical Plate Embedded Through Porous Medium," *Alexandria Engineering Journal*, **55**(3), 2125-2137.

<http://dx.doi.org/10.1016/j.aej.2016.06.024>

Khan, M.S., Karim, I., Ali, L.E., and Islam, A., 2012, "Unsteady MHD Free Convection Boundary-Layer Flow of a Nanofluid Along a Stretching Sheet with Thermal Radiation and Viscous Dissipation Effects," *International Nano Letters*, **2**(1), 24.

<http://dx.doi.org/10.1186/2228-5326-2-24>

Khan, M.S., Karim, I., and Biswas, M.H.A., 2012, "Non-Newtonian MHD Mixed Convective Power-Law Fluid flow over a Vertical Stretching Sheet with Thermal Radiation, Heat Generation and Chemical Reaction Effects," *Academic Research International*, **3**(3), 80-92.

Khan, M.S., Wahiduzzaman, M., Karim, I., Islam, M.S., and Alam, M.M., 2014, "Heat Generation Effects on Unsteady Mixed Convection Flow from a Vertical Porous Plate with Induced Magnetic Field," *Procedia Engineering*, **90**, 238-244.

<http://dx.doi.org/10.1016/j.proeng.2014.11.843>

Khan, N., and Mahmood, T., 2016, "Thermophoresis Particle Deposition and Internal Heat Generation on MHD Flow of an Oldroyd-B Nanofluid between Radiative Stretching Disks," *Journal of Molecular Liquids*, **216**, 571-582.

<http://dx.doi.org/10.1016/j.molliq.2016.01.074>

Krishnamurthy, M.R., Prasannakumara, B.C., Gireesha, B.J., and Gorla, R.S.R., 2016, "Effect of Chemical Reaction on MHD Boundary Layer Flow and Melting Heat Transfer of Williamson Nanofluid in Porous Medium," *Engineering Science and Technology, an International Journal*, **19**(1), 53-61.

<http://dx.doi.org/10.1016/j.jestch.2015.06.010>

Li, J., Liu, L., Zheng, L., and Bin-Mohsin, B., 2016, "Unsteady MHD Flow and Radiation Heat Transfer of Nanofluid In a Finite Thin Film with Heat Generation and Thermophoresis," *Journal of the Taiwan Institute of Chemical Engineers*, **67**, 226-234.

<http://dx.doi.org/10.1016/j.jtice.2016.07.022>

Mabood, F., Khan, W.A., and Ismail, A.I.M., 2015, "MHD Boundary Layer Flow and Heat Transfer of Nanofluids over a Nonlinear Stretching Sheet: a Numerical Study," *Journal of Magnetism and Magnetic Materials*, **374**, 569-576.

<http://dx.doi.org/10.1016/j.jmmm.2014.09.013>

Mabood, F., Shateyi, S., Rashidi, M.M., Momoniat, E., and Freidoonimehr, N., 2016, "MHD Stagnation Point Flow Heat and Mass Transfer of Nanofluids in Porous Medium with Radiation, Viscous Dissipation and Chemical Reaction," *Advanced Powder Technology*, **27**(2), 742-749.

<http://dx.doi.org/10.1016/j.apt.2016.02.033>

Madhava Reddy, C., Iyengar, T.K.V., and Krishna Gandhi, B., 2015, "Brinkman Model for Unsteady MHD Free Convection Flow of a Chemical Reacting Doubly Stratified Fluid with Heat Generation and Radiation," *Procedia Engineering*, **127**, 140-147.

<http://dx.doi.org/10.1016/j.proeng.2015.11.439>

Mahmoud, M.A.A., and Waheed, S.E., 2012, "MHD Flow and Heat Transfer of a Micropolar Fluid Over a Stretching Surface with Heat Generation (Absorption) and Slip Velocity," *Journal of the Egyptian Mathematical Society*, **20**(1), 20-27.

<http://dx.doi.org/10.1016/j.joems.2011.12.009>

Metri, P.G., Metri, P.G., Abel, S., and Silvestrov, S., 2016, "Heat Transfer in MHD Mixed Convection Viscoelastic Fluid Flow over a Stretching Sheet Embedded in a Porous Medium with Viscous

Dissipation and Non-Uniform Heat Source/Sink,” *Procedia Engineering*, **157**, 309-316.

<http://dx.doi.org/10.1016/j.proeng.2016.08.371>

Nachtsheim, P.R., and Swigert, P., 1995, “Satisfaction of the Asymptotic Boundary Conditions in Numerical Solution of the System of Non-Linear Equations of Boundary Layer Type,” NASA, TND-3004.

Nadeem, S., and Akram, S., 2010a, “Influence of Inclined Magnetic Field on Peristaltic Flow of a Williamson Fluid Model in an Inclined Symmetric or Asymmetric Channel,” *Mathematical and Computer Modelling*, **52**(1–2), 107-119.

<http://dx.doi.org/10.1016/j.mcm.2010.02.001>

Nadeem, S., and Akram, S., 2010b, “Peristaltic Flow of a Williamson Fluid in an Asymmetric Channel,” *Communications in Nonlinear Science and Numerical Simulation*, **15**(7), 1705-1716.

<http://dx.doi.org/10.1016/j.cnsns.2009.07.026>

Nadeem, S., Hussain, S.T., and L., C., 2013, “Flow of a Williamson Fluid Over a Stretching Sheet,” *Brazilian Journal of Chemical Engineering*, **30**(3), 619.

<http://dx.doi.org/10.1590/S0104-66322013000300019>

Nayak, M.K., Dash, G.C., and Singh, L.P., 2016, “Heat and Mass Transfer Effects on MHD Viscoelastic Fluid over a Stretching Sheet Through Porous Medium in Presence of Chemical Reaction,” *Propulsion and Power Research*, **5**(1), 70-80.

<http://dx.doi.org/10.1016/j.jprr.2016.01.006>

Pal, D., Mandal, G., and Vajravalu, K., 2016, “Soret and Dufour Effects on MHD Convective–Radiative Heat and Mass Transfer of Nanofluids over a Vertical Non-Linear Stretching/Shrinking Sheet,” *Applied Mathematics and Computation*, **287–288**, 184-200.

<http://dx.doi.org/10.1016/j.amc.2016.04.037>

Perdikis, C., and Raptis, A., 1996, “Heat Transfer of a Micropolar Fluid by the Presence of Radiation,” *Heat Mass Transfer*, **31**, 381-382.

<http://dx.doi.org/10.1007/BF02172582>

Ramzan, M., Bilal, M., and Chung, J.D., 2017, “MHD Stagnation Point Cattaneo–Christov Heat Flux in Williamson Fluid Flow with Homogeneous–Heterogeneous Reactions and Convective Boundary Condition — A Numerical Approach,” *Journal of Molecular Liquids*, **225**, 856-862.

<http://dx.doi.org/10.1016/j.molliq.2016.10.139>

Rashidi, M.M., Bagheri, S., Momoniat, E., and Freidoonimehr, N., 2016, “Entropy Analysis of Convective MHD Flow of Third Grade Non-Newtonian Fluid over a Stretching Sheet,” *Ain Shams Engineering Journal*.

<http://dx.doi.org/10.1016/j.asej.2015.08.012>

Reddy, P.S., and Chamkha, A.J., 2016, Soret and Dufour Effects on MHD Convective Flow of Al₂O₃–Water and TiO₂–Water Nanofluids Past a Stretching Sheet in Porous Media with Heat Generation/Absorption,” *Advanced Powder Technology*, **27**(4), 1207-1218.

<http://dx.doi.org/10.1016/j.apt.2016.04.005>

Rundora, L., and Makinde, O.D., 2015, “Effects of Navier Slip on Unsteady Flow of a Reactive Variable Viscosity Non-Newtonian Fluid through a Porous Saturated Medium with Asymmetric Convective Boundary Conditions,” *Journal of Hydrodynamics, Ser. B*, **27**(6), 934-944.

[http://dx.doi.org/10.1016/S1001-6058\(15\)60556-X](http://dx.doi.org/10.1016/S1001-6058(15)60556-X)

Salahuddin, T., Malik, M.Y., Hussain, A., Bilal, S., and Awais, M., 2016, “MHD Flow of Cattaneo–Christov Heat Flux Model for Williamson Fluid over a Stretching Sheet with Variable Thickness: Using Numerical Approach,” *Journal of Magnetism and Magnetic Materials*, **401**, 991-997.

<http://dx.doi.org/10.1016/j.jmmm.2015.11.022>

Sher Akbar, N., Ebaid, A., and Khan, Z.H., 2015, “Numerical Analysis of Magnetic Field Effects on Eyring-Powell Fluid Flow Towards a Stretching Sheet,” *Journal of Magnetism and Magnetic Materials*, **382**, 355-358.

<http://dx.doi.org/10.1016/j.jmmm.2015.01.088>

Si, X., Yuan, L., Zheng, L., Shen, Y., and Cao, L., 2016, “Lie Group Method for The Modified Model of MHD Flow and Heat Transfer of a Non-Newtonian Fluid with Prescribed Heat Flux over a Moving Porous Plate,” *Journal of Molecular Liquids*, **220**, 768-777.

<http://dx.doi.org/10.1016/j.molliq.2016.05.017>

Sravanthi, C.S., 2016, “Homotopy Analysis Solution of MHD Slip Flow Past an Exponentially Stretching Inclined Sheet with Soret-Dufour Effects,” *Journal of the Nigerian Mathematical Society*, **35**(1), 208-226.

<http://dx.doi.org/10.1016/j.jnms.2016.02.004>

Sreedevi, G., Raghavendra Rao, R., Prasada Rao, D.R.V., and Chamkha, A.J., 2016, “Combined Influence of Radiation Absorption and Hall Current Effects on MHD Double-Diffusive Free Convective Flow Past a Stretching Sheet,” *Ain Shams Engineering Journal*, **7**(1), 383-397.

<http://dx.doi.org/10.1016/j.asej.2015.11.024>

Srinivas, S., Subramanyam Reddy, A., Ramamohan, T.R., and Shukla, A. K., 2016, “Thermal-Diffusion and Diffusion-Thermo Effects on MHD Flow of Viscous Fluid Between Expanding or Contracting Rotating Porous Disks with Viscous Dissipation,” *Journal of the Egyptian Mathematical Society*, **24**(1), 100-107.

<http://dx.doi.org/10.1016/j.joems.2014.06.017>

Srinivasa, A.H., and Eswara, A.T., 2016, “Effect of Internal Heat Generation or Absorption on MHD Free Convection from an Isothermal Truncated Cone,” *Alexandria Engineering Journal*, **55**(2), 1367-1373.

<http://dx.doi.org/10.1016/j.aej.2016.04.003>

Turkyilmazoglu, M., 2012, “Dual and Triple Solutions for MHD Slip Flow of Non-Newtonian Fluid over a Shrinking Surface,” *Computers and Fluids*, **70**, 53-58.

<http://dx.doi.org/10.1016/j.compfluid.2012.01.009>

Umamaheswar, M., Raju, M.C., Varma, S.V.K., and Gireeshkumar, J., 2016, “Numerical Investigation of MHD Free Convection Flow of a Non-Newtonian Fluid Past an Impulsively Started Vertical Plate in the Presence of Thermal Diffusion and Radiation Absorption,” *Alexandria Engineering Journal*, **55**(3), 2005-2014.

<http://dx.doi.org/10.1016/j.aej.2016.07.014>

Vajravelu, K., Sreenadh, S., Rajanikanth, K., and Lee, C., 2012, “Peristaltic Transport of a Williamson Fluid in Asymmetric Channels with Permeable Walls,” *Nonlinear Analysis: Real World Applications*, **13**(6), 2804-2822.

<http://dx.doi.org/10.1016/j.nonrwa.2012.04.008>

Wang, C.Y., 1989, “Free Convection on a Vertical Stretching Surface,” *ZAMM - Journal of Applied Mathematics and Mechanics / Zeitschrift für Angewandte Mathematik und Mechanik*, **69**(11), 418-420.

<http://dx.doi.org/10.1002/zamm.19890691115>

Williamson, R.V., 1929, "The Flow of Pseudoplastic Materials," *Industrial and Engineering Chemistry Research*, **21(11)**, 1108.

<http://dx.doi.org/10.1021/ie50239a035>

Yadav, D., Nam, D., and Lee, J., 2016, "The onset of Transient Soret-Driven MHD Convection Confined within a Hele-Shaw Cell with Nanoparticles Suspension," *Journal of the Taiwan Institute of Chemical Engineers*, **58**, 235-244.

<http://dx.doi.org/10.1016/j.jtice.2015.07.008>

Zaidi, S.Z.A., and Mohyud-Din, S.T., 2016, "Analysis of Wall Jet Flow for Soret, Dufour and Chemical Reaction Effects in the Presence of MHD with Uniform Suction/Injection," *Applied Thermal Engineering*, **103**, 971-979.

<http://dx.doi.org/10.1016/j.applthermaleng.2016.03.086>

Zehra, I., Yousaf, M.M., and Nadeem, S., 2015, "Numerical Solutions of Williamson Fluid with Pressure Dependent Viscosity," *Results in Physics*, **5**, 20-25.

<http://dx.doi.org/10.1016/j.rinp.2014.12.002>

Zhang, Y., and Zheng, L., 2012, "Analysis of MHD Thermosolutal Marangoni Convection with the Heat Generation and a First-Order Chemical Reaction," *Chemical Engineering Science*, **69(1)**, 449-455.

<http://dx.doi.org/10.1016/j.ces.2011.10.069>

Zhao, J., Zheng, L., Zhang, X., and Liu, F., 2016, "Convection Heat and Mass Transfer of Fractional MHD Maxwell Fluid in a Porous Medium with Soret and Dufour Effects," *International Journal of Heat and Mass Transfer*, **103**, 203-210.

<http://dx.doi.org/10.1016/j.ijheatmasstransfer.2016.07.057>